Published in final edited form as:
Anal Chem. 2008 August 1; 80(15): 5847–5853. doi:10.1021/ac800317f.

Mass Spectrometry of Acoustically Levitated Droplets

Michael S. Westphall, **Kaveh Jorabchi**, and **Lloyd M. Smith***
Department of Chemistry, 1101 University Avenue, University of Wisconsin–Madison, Madison, Wisconsin 53706

Abstract

Containerless sample handling techniques such as acoustic levitation offer potential advantages for mass spectrometry, by eliminating surfaces where undesired adsorption/desorption processes can occur. In addition, they provide a unique opportunity to study fundamental aspects of the ionization process as well as phenomena occurring at the air–droplet interface. Realizing these advantages is contingent, however, upon being able to effectively interface levitated droplets with a mass spectrometer, a challenging task that is addressed in this report. We have employed a newly developed charge and matrix-assisted laser desorption/ionization (CALDI) technique to obtain mass spectra from a 5-μL acoustically levitated droplet containing peptides and an ionic matrix. A four-ring electrostatic lens is used in conjunction with a corona needle to produce bursts of corona ions and to direct those ions toward the droplet, resulting in droplet charging. Analyte ions are produced from the droplet by a 337-nm laser pulse and detected by an atmospheric sampling mass spectrometer. The ion generation and extraction cycle is repeated at 20 Hz, the maximum operating frequency of the laser employed. It is shown in delayed ion extraction experiments that both positive and negative ions are produced, behavior similar to that observed for atmospheric pressure matrix-assisted laser absorption/ionization. No ion signal is observed in the absence of droplet charging. It is likely, although not yet proven, that the role of the droplet charging is to increase the strength of the electric field at the surface of the droplet, reducing chargere combination after ion desorption.

Progress in the biological, medical, and pharmaceutical sciences has placed ever-increasing demands on technologies for handling and analyzing smaller and smaller sample volumes. Chip-based assays involving microfluidics have begun to address many of these demands.[1] In chip-based microfluidics, the surface-to-volume ratio increases as the fluid channel sizes decrease. As a result, nonspecific binding or adsorption of the analyte to the channel surfaces can become problematic, limiting the sensitivity of the desired assay.[2,3] One method of avoiding this issue is through containerless processing of samples using droplet levitation. Numerous containerless trapping techniques are becoming recognized for their ability to handle small volumes, serving as micromanipulators and microreactors.[4–6] Among these trapping techniques, single-axis acoustic levitation has gained wide acceptance because there are relatively few restrictions on the properties of the sample.[7] One of the most famous experiments involving droplet levitation was the Millikan oil drop experiment of 1909.[8] Since this early application to measure the electronic charge, e, droplet levitation has been used in various studies pertaining to the following: Brownian motion, photoemission, droplet evaporation, thermophoresis,[8] diffusion,[9] magnetization of superconducting particles,[10] Raman spectroscopy of microparticles,[11] live cell analysis,[5] protein crystallization,[12] preparing MALDI samples,[13] enzyme kinetics,[14] and more. A recent review by Priego-Capote and de Castro summarized the analytical techniques that have been implemented with an ultrasonically levitated droplet as, concentration by evaporation, liquid–liquid extraction, gas–liquid extraction, affinity two-phase separation, chemical derivatization, biochemical derivatization,

* To whom correspondence should be addressed. E-mail: smith@chem.wisc.edu. Fax (608) 265-6780.

crystallization, titration, and solvent exchange.[3] They also listed the in situ detection techniques implemented with an ultrasonically levitated droplet as photometry, fluorometry, phosphorimetry, Raman spectroscopy, surface-enhanced Raman scattering spectroscopy, and X-ray diffraction. Absent from this list, however, is mass spectrometry, although it has been employed as a off-line technique (a sample must be removed from the levitator and separately processed for mass spectral analysis).[15–18] Several techniques have been developed to generate gas-phase ions for mass spectrometry from droplets in motion;[19–22] however, none of these have been capable of ion generation from a levitated droplet.

Mass spectrometry has become a valuable tool for biologists and others in biotechnological fields. It has been employed to determine gene damage from environmental causes, identify structures of biomolecules, such as carbohydrates, nucleic acids, and steroids, sequence biopolymers such as proteins and oligosaccharides, determine how drugs are used by organisms, identify and quantify compounds of complex organic mixtures, and perform ultrasensitive multielement inorganic analyses.[23] Combining the power of mass spectrometry with acoustic levitation provides a new analytical approach to handling and analyzing small biological samples without loss of analyte to the walls during sample preparation and handling. In this report, we investigate in situ mass spectrometric analysis of acoustically levitated droplets. We use pulsed corona discharge along with time-resolved UV laser desorption and ion extraction to produce and extract ions from the levitator without disrupting the droplet.

EXPERIMENTAL SECTION

Ultrasonic Levitator

The single-axis acoustic levitator used for these experiments has been described previously[24] and implements the design principles outlined by Xie et al.[25,26] Briefly, the acoustic levitator consists of a single oscillating disk (sound wave emitter) and a concave reflector. Between the emitter and reflector a standing sound wave is formed. Located below the node of this wave is a region of high pressure capable of supporting a droplet. The emitter consists of a flat aluminum disk with a radius of 15.9 mm and is driven at 20 kHz with an acoustic transducer (Misonix, Farmingdale, NY). The acoustic reflector was constructed in-house from aluminum and has a spherical radius of 33.5 mm. The vertical spacing between the emitter and reflector is adjusted using a micrometer screw. The levitation force is tuned by adjusting the sound pressure level through the changing transducer input voltage or by adjusting the emitter–reflector spacing. The emitter–reflector spacing is maintained near 28 mm so that three nodes exist between the emitter and the reflector with the drop being levitated at the center node. The acoustic levitator was mounted to a XYZ translation stage to allow proper positioning of the levitated droplet/levitator relative to the mass spectrometer inlet nozzle.

Instrumental Setup

A schematic diagram of the instrumental setup employed is illustrated in Figure 1. The system consists of the levitator for containerless sample confinement, a corona ion source for droplet charging, ring electrodes to manipulate the electric fields surrounding the droplet, and a laser for sample desorption/ion generation. The levitator is positioned such that it will levitate the sample in the plane of the nozzle and 6 mm to the right or left of the nozzle entrance. This orthogonal geometry is adopted to facilitate the laser alignment for illuminating the area of the droplet closest to the MS nozzle. Two sets of ring electrodes with a 10-mm spacing are centered on the droplet. One set is parallel to the nozzle and the other is perpendicular to the nozzle. The ring electrodes are constructed from 26 AWG PVC hook-up wire with the PVC insulation removed. The electrodes are formed into 6-mm-diameter loops by bending the wire around a cylindrical mandrel. A corona discharge needle (1.5-mm-diameter stainless steel rod, sharpened and polished to a point) is placed on axis with the droplet and perpendicular to the

nozzle. The corona needle is housed in a 6-mm-diameter conducting cylinder, which extends 3 mm past the tip of the needle. The entire corona assembly is recessed 3 mm from the ring electrode pair perpendicular to the nozzle. The ring electrode between the droplet and the mass spectrometer nozzle acts as an ion gating electrode (gate ring electrode, Figure 1) while the other three ring electrodes shield the droplet from external electric fields including those due to the generation of the corona (guard ring electrodes, Figure 1). A conducting cylinder, placed around the needle, assists in formation of a stable corona discharge and shields the droplet from the electric field due to the corona needle. The small surface area of the ring electrodes did not sufficiently distort or block the acoustic field and, thus, had no deleterious effect on our ability to levitate the droplet.

An externally triggered 337-nm laser (5-ns pulse, NL100 nitrogen laser, Stanford Research Systems Inc., Sunnyvale, CA) was used for laser desorption from the levitated droplet. Light from the laser was focused to a 230-μm × 115-μm rectangular spot on the surface of the droplet closest to the MS inlet with a spherical fused-silica lens (2.54-cm diameter, 50-mm focal distance, Edmund Optics, Barrington, NJ). The laser output power was adjusted to 20 μJ using the high-voltage potentiometer on the laser and an adjustable iris placed in the laser beam path prior to the lens.

Mass spectral analysis was performed using an ESI-TOF instrument (Mariner, Applied Biosystems, Foster City, CA). The inlet nozzle of the instrument was modified with a stainless steel extension tube (5 cm long, 2 mm i.d.) to facilitate the levitator positioning and laser beam alignment with the levitated droplet. The voltages applied to the mass spectrometer nozzle, ring electrodes, and corona needle are all controlled independently, with the ability to pulse the potential on the corona needle and gate ring electrode between two independent values on a time scale of 5 μs. The ion gate ring electrode is pulsed between 100 and 3000 V using a high-voltage pulser (PVX-4140, Directed Energy Inc., Fort Collins, CO) in conjunction with two high-voltage power supplies (model PS350, Stanford Research Systems Inc.) set at 100 and 3000 V, respectively. The corona needle potential is switched between 6 kV (Series 205B high voltage supply, Bertan) and floating using a high-voltage relay (model W102VX-50, Struthers-Dunn). The guard ring electrode potentials were held at a constant 3000 V and the cylindrical corona shield at a constant 3500 V by a third Stanford Research high-voltage power supply and the application of a voltage divider. The mass spectrometer nozzle was kept at a constant 65 V. Pulsing of the ion gate ring, corona needle, and the firing of the laser were controlled with a National Instruments analog output board (PCI-6173) and an in-house LabView program.

Samples and Sample Preparation

The test solution used for this study is a mixture of the peptides MRFA (sequence, Met-Arg-Phe-Ala; average MW, 523.7), VAITVLVK (sequence, Val-Ala-Ile-Thr-Val-Leu-Val-Lys; average MW, 842.06), and bradykinin (sequence, Arg-Pro-Pro-Gly-Phe-Ser-Pro-Phe-Arg; average MW, 1060.19), which was obtained from Sigma-Aldrich. Each peptide was dissolved in 0.1% formic acid to yield 3 mM stock solutions. The liquid matrix is composed of a liquid support and a chro-mophore to absorb the UV laser light. The liquid support is prepared by mixing 1:1 volumetric ratios of diethanolamine and 50% ethanol. To this, α-cyano-4-hydroxycinnamic acid is added to a concentration of 600 mM. The resulting solution is sonicated for 15 min and then vortexed for 1 min prior to use. The sample for analysis is prepared by diluting the peptide stock solutions with the liquid matrix to obtain a concentration of 100 μM for each peptide. HPLC grade water was purchased from J. T. Baker and 200-proof ethanol was from Pharmaco-AAper. All other materials were purchased from Sigma-Aldrich and used with no further purification.

Safety Considerations

Caution and standard safety procedures should be used when employing the above experimental apparatus. Particularly, extreme caution must be taken to avoid contact with high-voltage rings and to protect the eyes from stray UV light.

RESULTS AND DISCUSSION

Gas-Phase Ion Generation, Ion Extraction, and Analytical Performance

Acoustic levitation is the only levitation technique that depends solely on the material density and not the object size, electrical charge, or refractive index.[2] This makes it ideal for containerless mass spectral sample analysis where the charge and size of the levitated object may be subject to change. One of the challenges faced in coupling mass spectrometry with acoustic levitation is keeping the droplet stable in the presence of the strong electric fields required for ion generation and transport from the levitator to the mass spectrometer. Since we wish to focus the ions into the mass spectrometer, nonuniform electric fields are employed. These fields will produce a dielectrophoretic force on the droplet in the direction of the electric field gradient.[27] This issue is further exacerbated by the choice to use a single-axis levitator where interfacing to the mass spectrometer is most easily accomplished with the inlet to the mass spectrometer perpendicular to the axis of levitation. The restoring force to the droplet is 2.5 times less in the radial direction than in the longitudinal direction or parallel to the axis of levitation.[28] To enable analyte ionization without the loss of the droplet from the levitator, we employed the recently developed technique of charge and matrix-assisted laser desorption/ionization mass spectrometry (CALDI).[29] With this technique, the droplet is charged prior to laser desorption by exposure to corona ions. Relative to atmospheric pressure matrix-assisted laser desorption (AP-MALDI), precharging the droplet reduces the external field strength needed for ion production significantly (up to 1 order of magnitude), with no loss of signal intensity.[29] Exposure to the external fields was also minimized through pulsing of the potentials, as further described below.

Figure 2 displays a mass spectrum collected from the three-peptide mixture described above. The spectrum is an average of 10 separate spectra, where each spectrum was collected over a 3-s time period. A 5-μL droplet of the liquid MALDI matrix and analyte mix was levitated by depositing the droplet into the levitator off the end of a syringe. The four ring electrodes and the corona source were set in place prior to levitating the droplet. As mentioned above, in lieu of applying a continuous electric field to the droplet, a series of short voltage pulses were used, minimizing the time for which the droplet was exposed to electrostatic forces. Figure 3 summarizes a typical pulsing cycle. First, a 5-ms corona charging period (ion gate ring set at 100 V, guard ring set at 3000 V, and corona needle set at 6000 V) is employed to charge the droplet, Figure 3A. Next a 5-ms field-free relaxation time (all ring electrodes placed at 3000 V) is invoked, allowing the droplet to restabilize within the trap, Figure 3B. Ion generation and extraction occurs with the application of an ion extraction potential (ion gate ring set at 100 V, corona and guard rings set at 3000 V, corona needle floating) for 3 ms during which time the laser was fired, Figure 3C. This scenario was repeated at a 20-Hz repetition rate with the generated ions being analyzed on a Mariner ESI-TOF instrument. It is important to note that the potential placed across the droplet is the same during the charging and ion extraction period. When CALDI experiments were performed on liquid MALDI droplets supported on Teflon post, it was noted that the presence or absence of corona ions during the laser pulsing had no effect on the observed ion signal.[29] We have observed the same behavior when utilizing levitated droplets. Thus, employing a pulse sequence where the laser is fired 4 ms into the 5-ms charging period (separate analyte ion generation and extraction periods not employed) yields results identical to the longer cycle employing separate charging, extraction, and relaxation periods. This particular pulsing sequence has the advantage that it minimizes the

total time that the droplet is in the presence of a strong electric field, helping to ensure the stability of the droplet within the acoustic levitator. Initial data were collected using the long cycle (data not shown) while all the data presented in this paper were obtained using the shorter cycle.

The maximum time a droplet was retained in the levitator for these studies was 6 h, at which point the sample was removed by reducing the levitator power. Figure 4 illustrates the signal stability of the generated ion signal from a levitated droplet containing MRFA and liquid matrix over a 20-min period. The total ion current chromatogram was obtained by integrating the signal over the mass range of 522–528 Da (isotopic peaks of MRFA) for 30-s intervals. Fitting a line to the data reveals an average drop in signal of 32 counts out of 7000 counts over a 1-min period, or a signal loss of less than 0.5%/min. No adjustments were made to the levitator, potential pulsing cycle, or mass spectrometer during the20-min test period. This represents very good long-term stability, consistent with the high ion current stabilities observed with liquid MALDI matrixes.[30]

Mechanistic Considerations

Ionization and the Role of Excess Charge—Charging of the droplet prior to laser desorption is essential for the in situ mass spectral detection of ions from a droplet supported in a single-axis levitator reported here. At no point were we able to find voltage levels that would allow the observation of analyte ions after laser desorption if the droplet was not first charged. The high-voltage levels applied to the rings would result in either the loss of the droplet from the levitator or the emission of corona ions from the ring electrodes.

To achieve the best analytical performance in terms of sensitivity and reproducibility, it is desired to charge the droplet to the maximum possible level. The external electric field plays a significant role in adding sufficient charge to the droplet prior to desorption. The maximum charge that can be absorbed by a spherical droplet in an electric field containing monopolar ions is governed by the Pauthenier equation: [31]

$$Q_{\max} = 12\pi\varepsilon r^2 E_0 \quad (1)$$

where ε is the permittivity of free space. From the above equation it can be seen that the maximum charge that can be placed on the droplet is a function of the droplet radius r and the strength E_0 of the electric field in which the droplet is placed. It is independent of the ion type or density impinging upon the droplet. However, the type of ion and ion density used in the charging, as well as the conductivity of the droplet, do affect the rate of charging, which has a hyperbolic time dependence.[32] This hyperbolic time dependence is such that although the initial rate of charging is high (order of milliseconds), it soon falls off, taking seconds to reach saturation. Charge measurements conducted on an electrically isolated droplet on a Teflon post revealed that a single corona event of 5-ms duration charges the droplet to a level slightly higher than 50% of the saturation point achieved by 500, 5-ms corona pulses (data not shown). The data shown above were collected at 1 charging event per laser shot in the interest of maximizing the desorption repetition rate, thus, the sensitivity.

As for ESI and MALDI, for which many aspects of the desorption–ionization process are not yet well understood, the role of the excess charge placed on the droplet is not easily deciphered. However, all of our data to date strongly suggest that the method of ion generation is a MALDI-related phenomenon and that the excess charge placed on the droplet is primarily aiding in the prevention of ion recombination. These results are discussed below.

Berkout et al.[33] have modeled the ionization process in AP-MALDI as the ejection of a plume of positive and negative ions by the laser pulse. This is followed by ions drifting to the nozzle

under the influence of an electric field and gas flow. During the initial stages of plume expansion, the positive ions can recombine with negative ions (ion recombination). The application of an electric field can aid in separation of the negative and positive ions, minimizing the effects of ion recombination. Berkout et al. also reported experimental results showing that delaying the presence of an electric field by 3–4 μs after the laser pulse resulted in a factor of 3 depletion in the ion signal due to ion recombination compared to pulsing the laser with the electric field present. We have observed similar results with a charged levitated droplet, as seen in Figure 5, where the signal intensity quickly diminishes with increasing delay time between the laser pulse and external electric field. This experiment suggests that laser desorption from a positively charged droplet results in generation of both positive and negative ions, similar to what is obtained from a neutral droplet in AP-MALDI. A difference between the two approaches, as pointed out earlier, is that the magnitude of the external electric field required for ion generation is reduced for a charged droplet, although an external field is still required at the time of the laser pulse for maximum signal generation.

Droplet Charging by Laser Desorption

On the basis of the ion generation mechanism described above, one can postulate that the negative ions created by the laser pulse recombine with the droplet under the influence of the electric field employed to extract the positive ions. Accordingly, the excess positive charge on the droplet is reduced by each laser shot. This could eventually lead to charge reversal on the droplet by repeated illumination in the absence of recharging by corona ions. We tested this hypothesis on a levitated droplet and in fact observed such a charge reversal for a droplet that was charged by a single pulse of corona ions and then illuminated several times by the laser. The polarity of the excess charge on the droplet is easily determined by monitoring the dislocation of the charged droplet when exposed to an electric field.

Selectively extracting ions of a given polarity can also be used to charge the droplet to the opposite polarity for mass spectrometric analysis. For positive ion detection, we reversed the polarity of the rings so that the negative ions were extracted and the positive ions recombine with the droplet upon laser illumination. Note that the number of positive ions created from a neutral or negatively charged droplet by a single laser shot is not large enough to be detected by the Mariner mass spectrometer. However, these positive ions can be collected in the droplet over several laser shots, resulting in an excess positive charge on the droplet similar to that produced by application of a positive corona ion pulse. After the laser-charging step, we switched the polarity of the ring electrodes to extract and detect the positive ions from the positively charged droplet. Figure 6 compares the total ion chromatograms from the same droplet using two charging methods. The charging was effected either by laser firing and negative ion extraction at 20 Hz for 30 s or by a single 5-ms pulse of corona ions. The droplet was then analyzed by the same laser pulsing and ion extraction sequences described in the Experimental Section. Mass spectra were recorded at the rate of 1 spectrum/s until no signal was detected by the MS. The figure includes two replicates of each charging method to illustrate the reproducibility. The averaged mass spectra and ion currents for the two charging methods are very similar. This could be a consequence of near-saturation charging. In addition, our charge measurements for a droplet on a Teflon post shows that only a small fraction (<30%) of the original charge on the droplet is consumed before the signal falls below the detection limit of the MS (data not shown), further signifying the importance of excess charge on the droplet.

CONCLUSION

We have successfully interfaced mass spectrometry with acoustic droplet levitation through the introduction of charge/matrix-assisted laser desorption/ionization. By precharging the

droplet prior to laser ablation, we were able to minimize the electric field strengths to which the droplet was exposed, enabling the extraction of peptide analyte ions without disruption of the levitated droplet. The mechanism through which the additional charge aids in the generation of analyte ions was examined but remains ambiguous. The generated data support our assumption that the excess charge on the droplet enhances the local electric field, reducing the rate of ion recombination. To further the utility of this technique, we plan to implement an IR laser, which will allow the removal of matrix and chromophore molecules from the sample solution, minimizing any ion suppression effects. Lastly, we will employ this support/substrate-free MALDI technique to make direct comparisons with MALDI samples placed on various different sample supports (stainless steel, Teflon, paraffin, etc.). Combined with charge/matrix-assisted laser desorption/ionization, this system provides a unique probe to investigate the interaction of the laser with the sample support, which is known to affect the analyte signal.[34]

Acknowledgements

This work was supported by the National Heart, Lung, and Blood Institute's (NHLBI) Proteomics Program (NO1-HV-28182), and by NIH grant R33DK070297.

References

1. Felton MJ. Anal Chem 2003;75:505A–508A.
2. Santesson S, Nilsson S. Anal Bioanal Chem 2004;378:1704–1709. [PubMed: 14762640]
3. Priego-Capote F, de Castro L. Trac-Trends Anal Chem 2006;25:856.
4. Kavouras A, Krammer G. Rev Sci Instrum 2003;74:4468–4473.
5. Santesson S, Andersson M, Degerman E, Johansson T, Nilsson J, Nilsson S. Anal Chem 2000;72:3412–3418. [PubMed: 10952520]
6. Vandaele V, Lambert P, Delchambre A. Precis Eng: J Int Soc Precis Eng Nanotechnol 2005;29:491–505.
7. Welter E, Neidhart B. Fresenius J Anal Chem 1997;357:345–350.
8. Davis EJ. Aerosol Sci Technol 1997;26:212–254.
9. Davis EJ, Chorbaji E. Ind Eng Chem Fundam 1974;13:272–277.
10. Grader GS, Hebard AF, Eick RH. Appl Phys Lett 1988;53:2238–2240.
11. Thurn R, Kiefer W. Appl Spectrosc 1984;38:78–83.
12. Chung SK, Trinh EH. J Cryst Growth 1998;194:384–397.
13. Bogan MJ, Agnes GR. Anal Chem 2002;74:489–496. [PubMed: 11838665]
14. Weis DD, Nardozzi JD. Anal Chem 2005;77:2558–2563. [PubMed: 15828793]
15. Haddrell AE, Feng X, Nassar R, Bogan MJ, Agnes GR. J Aerosol Sci 2005;36:521–533.
16. Bogan MJ, Bakhoum SFW, Agnes GR. J Am Soc Mass Spectrom 2005;16:254–262. [PubMed: 15694775]
17. Bogan MJ, Agnes GR. Rapid Commun Mass Spectrom 2004;18:2673–2681. [PubMed: 15476188]
18. Bogan MJ, Agnes GR. J Am Soc Mass Spectrom 2004;15:486–495. [PubMed: 15047054]
19. Grimm RL, Beauchamp JL. J Phys Chem B 2005;109:8244–8250. [PubMed: 16851963]
20. Grimm RL, Beauchamp JL. J Phys Chem B 2003;107:14161–14163.
21. Hager DB, Dovichi NJ. Anal Chem 1994;66:1593–1594.
22. Hager DB, Dovichi NJ, Klassen J, Kebarle P. Anal Chem 1994;66:3944–3949.
23. Chiu, CM.; Muddiman, DC. American Society for Mass Spectrometry: Education. 2001.
24. Hilger RT, Westphall MS, Smith LM. Anal Chem 2007;79:6027–6030. [PubMed: 17580951]
25. Xie WJ, Cao CD, Lu YJ, Wei B. Phys Rev Lett 2002:89.
26. Xie WJ, Wei B. Phys Rev E 2002:66.
27. Kralj JG, Lis MTW, Schmidt MA, Jensen KF. Anal Chem 2006;78:5019–5025. [PubMed: 16841925]
28. Stephens TL, Budwig RS. Rev Sci Instrum 2007:78.

29. Jorabchi K, Westphall MS, Smith LM. J Am Soc Mass Spectrom. In press
30. Palmblad M, Cramer R. J Am Soc Mass Spectrom 2007;18:693–697. [PubMed: 17223354]
31. Inculet II, Adamiak K. IEEE Trans Ind Appl 1993;29:1058–1061.
32. Adamiak K. IEEE Trans Ind Appl 2002;38:1001–1007.
33. Berkout VD, Kryuchkov SI, Doroshenko VM. Rapid Commun Mass Spectrom 2007;21:2046–2050. [PubMed: 17535019]
34. Frankevich VE, Zhang J, Friess SD, Dashtiev M, Zenobi R. Anal Chem 2003;75:6063–6067. [PubMed: 14615982]

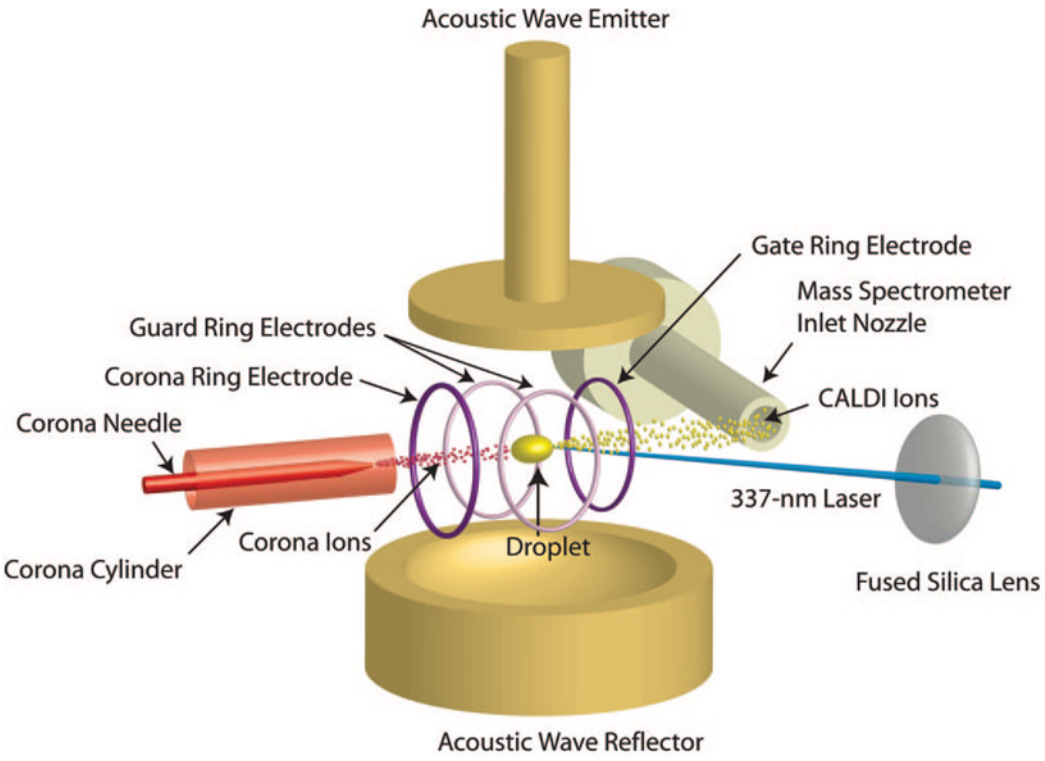

Figure 1.
Experimental setup used to generate levitated droplet CALDI spectra. The mass spectrometer nozzle is orthogonal to the ion generation and extraction axis.

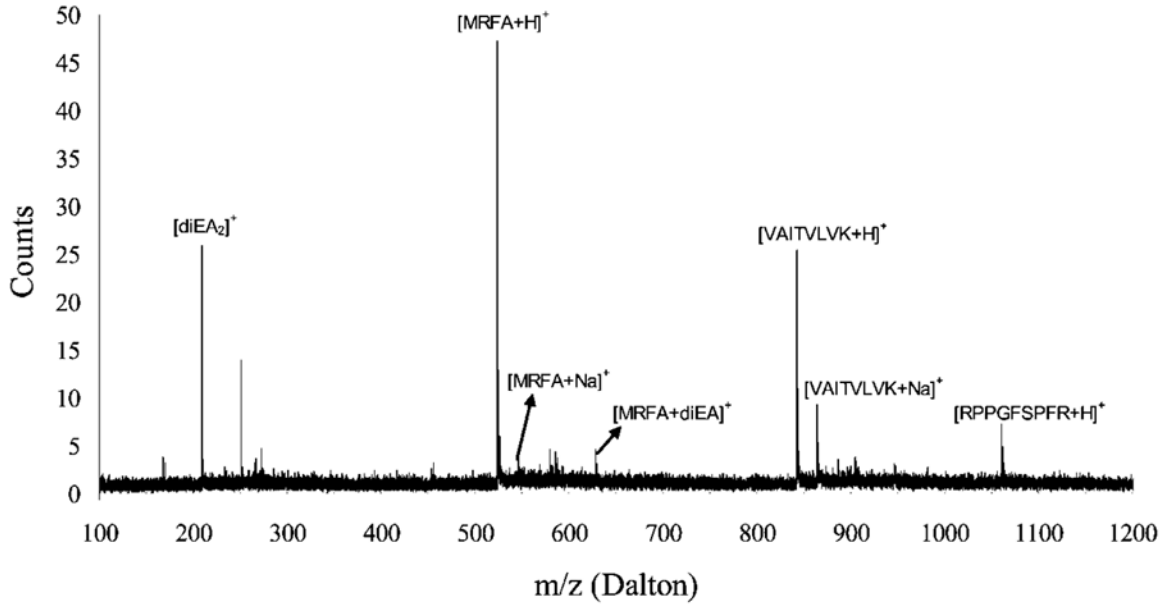

Figure 2.

Mass spectrum obtained from an acoustically levitated droplet containing a liquid matrix (see text for details) and a three-peptide mixture: MRFA (sequence, Met-Arg-Phe-Ala; average MW, 523.7), VAITVLVK (sequence, Val-Ala-Ile-Thr-Val-Leu-Val-Lys; average MW, 842.06), and bradykinin (sequence, Arg-Pro-Pro-Gly-Phe-Ser-Pro-Phe-Arg; average MW, 1060.19) at a concentration of 100 μM each. The data is an average of 10 separate spectra, where each spectrum was collected over a 3-s time period.

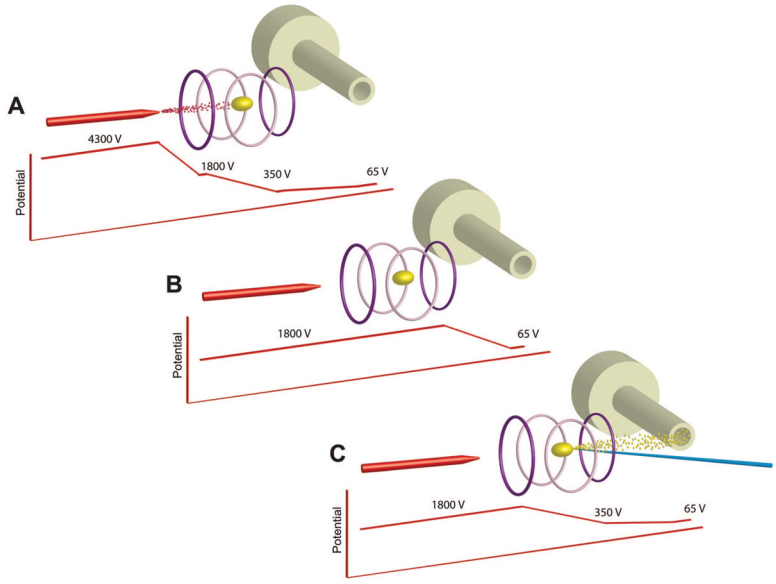

Figure 3.

Sequence of ion generation: (A) pulsed corona ion generation to charge droplet, (B) droplet stabilization period, and (C) laser desorption, ion generation, and extraction. The cycle A–B–C is repeated at 20 Hz. Below each sequence is a potential line representing the voltages applied to each of the components. The levitator and the two guard ring electrodes have been eliminated for figure clarity.

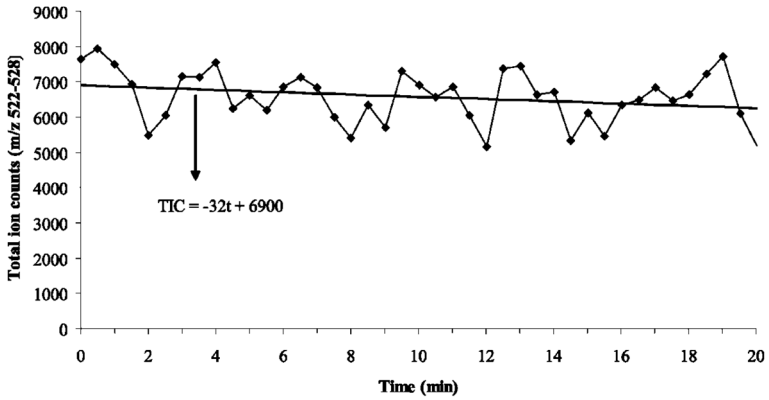

Figure 4.

Total ion current chromatogram obtained by integrating the signal over the mass range of 522–528 Da (isotopic peaks of MERFA) at 30-s intervals over a 20-min period. The linear fit shown corresponds to an average drop in signal of 32 counts out of 7000 over a 1-min period.

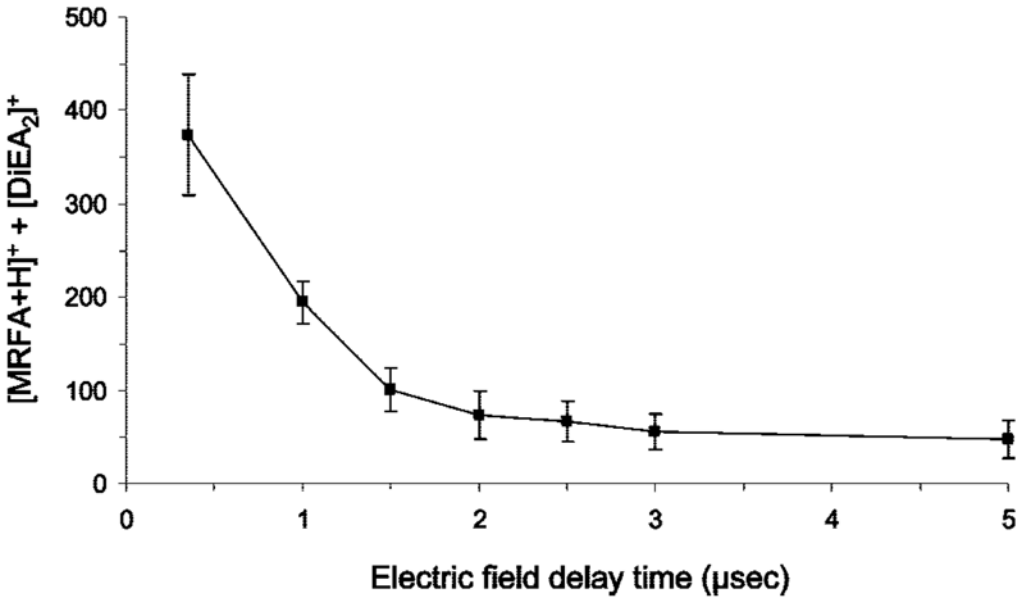

Figure 5.
MRFA peptide signal as a function of delay time between the nitrogen laser pulse and application of a 2.9 kV/cm electric field to aid in ion extraction.

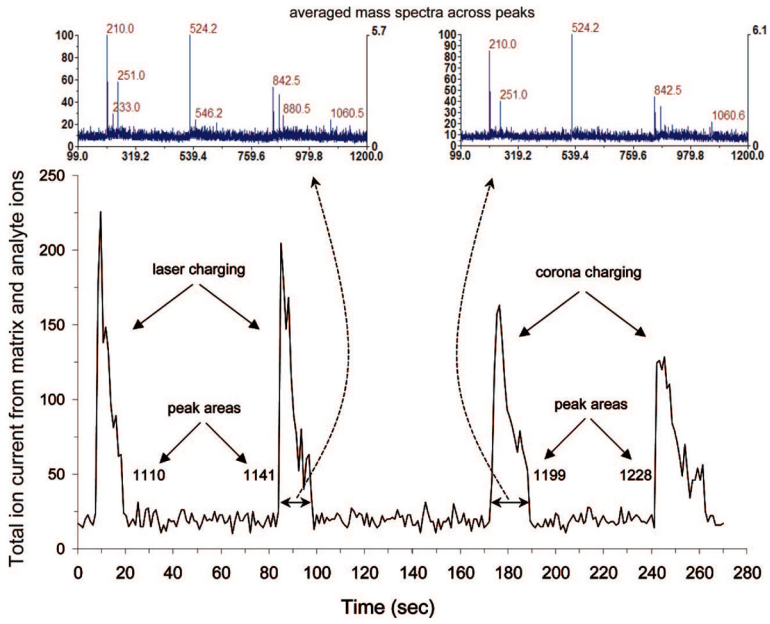

Figure 6.
Total ion chromatograms from the same droplet using either laser (left side) or corona (right side) charging of the droplet.